Article

Imaging Hg2+-induced oxidative stress by NIR molecular probe with “dual-key-and-lock” strategy

Xiaopeng Yang, xiaojing han, yongru zhang, jianfei liu, Jun Tang, Di Zhang, yufen zhao, and Yong Ye

Anal. Chem., **Just Accepted Manuscript** • DOI: 10.1021/acs.analchem.0c02509 • Publication Date (Web): 31 Jul 2020

Imaging Hg^{2+}-induced oxidative stress by NIR molecular probe with "dual-key-and-lock" strategy

Xiaopeng Yang[a], Xiaojing Han[a], Yongru Zhang[a], Jianfei Liu[a], Jun Tang[a], Di Zhang[b, *], Yufen Zhao[a, c], Yong Ye[a,*]

[a] Green Catalysis Center, and College of Chemistry, Zhengzhou University, Zhengzhou 450001, China. *Corresponding author, E-mail: yeyong03@tsinghua.org.cn

[b] Institute of Agricultural Quality Standards and Testing Technology, Henan Academy of Agricultural Sciences, Zhengzhou 450002, China. E-mail: pandy811@163.com

[c] Institute Drug Discovery Technology, Ningbo University, Ningbo 315211, Zhejiang, China

ABSTRACT: Mercury (Hg) is considered as an extremely toxic heavy metal which is extremely harmful to both the human body and environment. In addition, Hg^{2+}-induced oxidative stress also exerts a crucial role to play in pathophysiological mechanisms of mercury toxicity. Thus, the efficient and specific fluorescent probes for imaging Hg^{2+}-oxidative stress are necessary. In the present study, we rationally design a novel Hg^{2+}-activated and ICT-based NIR emission fluorescent probe **NIR-HO** for sequentially monitoring $ONOO^-$ level with "dual-key-and-lock" strategy. The probe **NIR-HO** showed rapid response, excellent specificity and sensitivity for the detection of Hg^{2+} and $ONOO^-$ in vitro. Cells imaging demonstrated that Hg^{2+}-induced oxidative stress was involved in $ONOO^-$ upregulation. Besides, GSH, NAC and EDTA were employed as excellent detoxifying drug against Hg^{2+}-induced toxicity. Moreover, the probe **NIR-HO** was successfully used for imaging Hg^{2+} and $ONOO^-$ in vivo. In brief, **NIR-HO** provides a simple and powerful approach which can be used to image Hg^{2+}-induced oxidative stress in the pathological environment.

Introduction

It is acknowledged that mercury (Hg) is a highly poisonous heavy metal, which has been considered as the major threat to human health.[1] Hg is usually transferred into the human body through the food chain and deposited, and then cause chronic poisoning which has been proven to lead to liver, kidneys, brain, stomach and nerve damage.[2-4] Nevertheless, the relevant pathogenesis of Hg^{2+} chronic poisoning has not been clear. Recently, Hg^{2+} was dementated to show a strong affinity for the mercapto (SH)-containing complexes in human body, which can cause the sulfhydryl groups of proteins, enzymes and lipids to agglomerate.[5, 6] Besides, the explosion of ROS caused by oxidative stress may be closely associated with mercury-induced toxicity.[7, 8] Increasing intracellular Hg^{2+} concentrations usually leads to NO and $O_2^{\cdot-}$ bursting as well as deactivate the antioxidants in the body by connecting with the mercapto (-SH) group. $O_2^{\cdot-}$ reacts rapidly with NO to generate peroxynitrite ($ONOO^-$).[9] In life system, as strong oxidant and nucleophile[10-16], Hg^{2+}-induced $ONOO^-$ can directly interact with proteins, lipids, DNA by oxidation, and can also be converted to other ROS including hydroxyl radicals, carbonate radicals, and nitrogen dioxide.[17-19] Actually, mis-regulation of $ONOO^-$ levels often causes various diseases including stroke, heart disease, neurodegenerative disease, cardiovascular disease, inflammation and cancer.[20-25] However, abnormal changes of $ONOO^-$ level caused by Hg^{2+}-induced oxidative stress still remain unclear due to its short life, highly active, and low level.[26] Moreover, the precise mechanism of Hg^{2+} and $ONOO^-$ in the biological environment is not completely known.[27, 28] Thus, the development of efficient methods and technologies to monitor the Hg^{2+}-induced oxidative stress would be conductive to deeply understanding the biological role of Hg^{2+} -induced diseases.

Due to its low cost, low radioactivity, high sensitivity and rapidly catch information of activated species in the biological environment in combination with fluorescent imaging technology, fluorescent probes have been extremely employed to reveal the physiological activities of metal ions, anions, enzyme, ROS, RSS and RNS.[29-36] In particular, near-infrared (NIR) emission at 650-900 nm fluorescent probes have advantages associated with maximizing tissue penetration, avoiding biological background fluorescence and less damage, and consequently have attracted extensive attention of chemist.[37-43] To detect $ONOO^-$ or Hg^{2+}, many of fluorescent probes have been reported.[44-51] However, most of probes for Hg^{2+} and $ONOO^-$ are developed based on "one-key-and-lock" strategy whose fluorescent signals are switched on by one "key" Hg^{2+} or $ONOO^-$ (Scheme 1A).[52-59] Designing a probe, whose emission can only be switched on in the presence of two "keys" Hg^{2+} and $ONOO^-$, is better for specifically studying the process of Hg^{2+}-induced $ONOO^-$ generation with "dual-key-and-lock" strategy[60-63]. As a result, developing a simple, NIR-emission and powerful molecular probe for meeting the needs of monitoring Hg^{2+} and $ONOO^-$ is necessary to study.

To realize the visual imaging of Hg^{2+}-induced $ONOO^-$ generation, we designed and synthesized a novel Hg^{2+}-activated and near-infrared emission fluorescent probe **NIR-HO** based on ICT for detecting Hg^{2+} and $ONOO^-$ with "dual-key-and-lock" strategy and "AND" logic gate (Scheme 1B, C). The diphenylphosphinothioyl moiety was introduced into NIR emission fluorophore to achieve high efficiency, sensitivity and selectivity detection of Hg^{2+} and $ONOO^-$. At first, the P=S of thiophosphinate was oxidized by Hg^{2+} to P=O; Then $ONOO^-$ would promote cleavage of the phosphinate ester P–O bond in **NIR-Hg** to produce **NIR-ONOO**.[3, 64-66] When the P–O bond was broken by $ONOO^-$, the NIR emission enhanced. In addition, the probe was proved to be highly selective for monitoring Hg^{2+} and $ONOO^-$ in the biological system. More importantly, we found that Hg^{2+} can cause oxidative stress and generate peroxynitrite ($ONOO^-$) from cell imaging for the first time. These results might provide a guiding significance to deeply study the pathological mechanisms of Hg-induced diseases and death.

Scheme 1. A) Design strategy of previous probes; B) The truth table of NIR-HO; C) Response mechanism of probe NIR-HO.

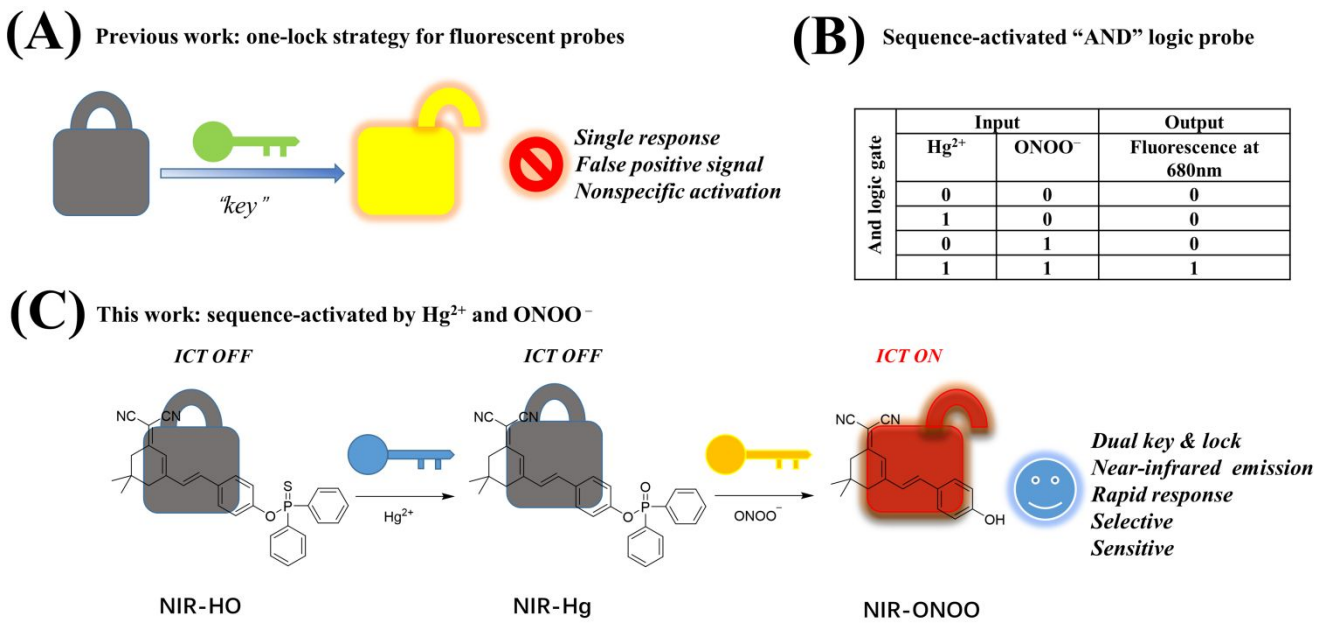

Experimental

Synthesis. Intermediates compounds **1** and **2** were synthesized based on published procedures[67, 68].

Preparation of **NIR-HO**: Compound **2** (290.4 mg, 1 mmol) was dissolved in THF (10 ml) with triethylamine (152.0 mg, 1.5 mmol), and then compound 1 (379.0 mg, 1.5mmol) was added at 0 °C, and stirred 12 hours at room temperature. Then removing THF by evaporation, the remaining solid was purified by silica column chromatography and recrystallization to provide a yellow solid 435.7 mg NIR-HO with 86% yield. ^{1}H NMR ($CDCl_3$, 400 MHz): δ = 8.01 (m, 4H), 7.55 (m, 6H), 7.41 (d, J = 8.6 Hz, 2H), 7.10 (m, 2H), 7.00 (d, J = 16.1 Hz, 1H), 6.88 (d, J = 16.1 Hz, 1H), 6.82 (s, 1H), 2.61 (s, 2H), 2.45 (s, 2H), 1.09 (s, 6H) ppm; ^{13}C NMR ($CDCl_3$, 100 MHz): δ =169.3, 153.7, 151.7 (J = 8.8 Hz), 136.0, 134.0 (J = 110.2 Hz), 132.4 (J = 4.6 Hz), 131.4 (J = 11.6 Hz), 128.9, 128.7, 128.6 (J = 13.6 Hz), 123.5, 122.4 (J = 5.1 Hz), 113.1 (J = 78.2 Hz), 78.7, 43.0, 39.2, 32.0, 28.0 ppm; ^{31}P NMR (162 MHz, $CDCl_3$): δ = 82.8 ppm; Mp: 201-202 °C; HR-MS: m/z calcd for $[C_{31}H_{27}N_2OPS]^+$ =507.1654, Found: 507.1654.

Cytotoxicity assays. Cytotoxicity assays were performed by using Cell Counting Kit-8 (CCK-8) in accordance with our previously reported. The cells were treated with probe **NIR-HO** (0-20 μM) for 24 hours, and the cell cytotoxicity was determined by CCK-8 analysis.

Cell Culture and Imaging. MCF-7 cells were cultured in RPMI-1640 supplemented with 10% fetal bovine serum, at 37.0 °C, in 5% CO_2. Cells were plated on culture dish and allowed to adhere for 24 hour. Before carrying out the experiments, the media was removed and the cells were washed three times with PBS buffer (pH 7.4). Cells were imaged with the application of Leica TCS SP8 confocal microscope. (excitation: 552 nm emission: 640-720 nm)

Mice imaging. Before imaging, the Kunming mice were fasted for 12 hours to avoid possible food fluorescence interference to the dye fluorescence. The mice were classified into two groups. The first group was given an injection of **NIR-HO** (10 μM, 100 μL) for 0.5 hour and then given an injection of PBS (100 μL) and was imaged after 0.5 hour. Followed by subcutaneously injection with Hg^{2+} and $ONOO^-$ (100 μL, 10 μM), the second group was given an injection of **NIR-HO** (10 μM, 100 μL) for 0.5 hour, and was imaged after 0.5 hour. Before imaging, the mice were anesthetized with 4% chloral hydrate (15 mL/kg) by intraperitoneal injection. Then, whole body images of the mice were acquired using an IVIS Lumina III system with channel (560-nm excitation and 670-nm emission).

Scheme 2. Synthetic route of probe **NIR-HO**.

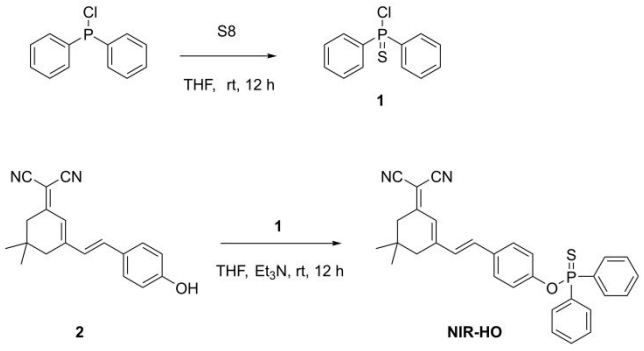

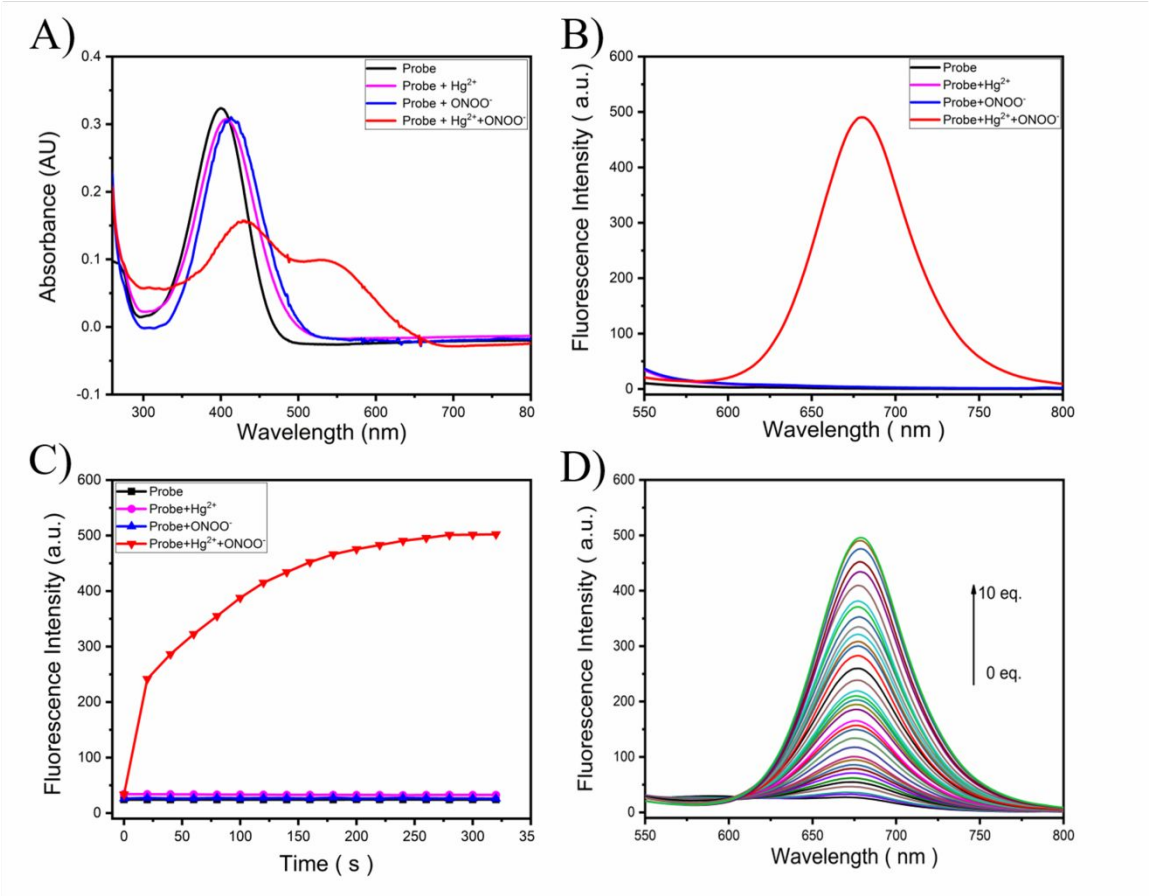

Figure 1. A) The absorption spectra. B) Fluorescence emission spectra of NIR-HO (10 μM) toward Hg^{2+} and $ONOO^-$ (10 equiv.). C) Time-dependent intensity at 680 nm of NIR-HO (10.0 μM) to Hg^{2+} and $ONOO^-$ (10 equiv.). D) Fluorescence titrations spectra of NIR-HO (10.0 μM) toward $ONOO^-$ in the presence of 10 equiv. Hg^{2+}. (PBS/EtOH=4/6, v/v, 10 mM, pH 7.4, 25 °C, Ex = 550 nm)

Results and discussion

Design and Synthesis of NIR-HO. In order to achieve specific detection of Hg^{2+}-induced oxidative stress, it is urgently needed to develop an efficient tool for Hg^{2+} and $ONOO^-$ combined detection. We choose "dual-key-and-lock" strategy to apply for probe designing. The thiophosphinate ester moiety can be used as a "lock" with two "keys" Hg^{2+} and $ONOO^-$. Meanwhile, near-infrared emission fluorophore serves as the reporting signal part. Furthermore, probe **NIR-HO** can be easily synthesized in a few steps as depicted in Scheme 2. The NMR and HR-MS spectroscopy of probe **NIR-HO** were shown in supplementary data (Figure S1-4).

Spectroscopic response of NIR-HO. When obtaining the designed probe, we studied the sensing ability of **NIR-HO** (10 μM) towards Hg^{2+} and $ONOO^-$ in PBS buffer (H_2O/EtOH=4/6, v/v) at first. Probe **NIR-HO** (Φ = 0.01) presented weakly fluorescence emission at 680 nm and absorption center at 410 nm from fluorescence emission and absorption spectra (Figure 1A, B). With only 10 equiv. of Hg^{2+} added, the emission showed a negligible change, and the absorption center shifted to 420 nm. Moreover, there also existed no change of fluorescence responses and absorption after only addition of 10 equiv. $ONOO^-$. When both Hg^{2+} and $ONOO^-$ were added, the fluorescence intensity gradually increased to a quantum yield of Φ = 0.16. At the same time, two new absorptions at 440 and 550 nm appeared (Figure 1B). The time dependence of the emission profile of was measured via recording changes in emission at 680 nm towards Hg^{2+} and $ONOO^-$. Obviously, no obvious change of fluorescence emission intensity could be found after the addition of Hg^{2+} or $ONOO^-$ within 5 minutes (Figure 1C). However, the emission showed significant enhancement and reached maximum plateau value within 5 minutes after simultaneously adding Hg^{2+} and $ONOO^-$. As shown in Figure 1D, We further investigated the fluorescent titration experiment. At first, we added 10 equiv. of Hg^{2+} to solution for activating **NIR-HO**, and the fluorescence emission intensity was gradually enhanced and rose to platform emission intensity with different concentration $ONOO^-$ 0-100 μM. According to Figure S5, the emission intensity (680 nm) indicated a good linear relationship to $ONOO^-$ concentration (R^2 = 0.9974). Afterwards, the limit of detecting for $ONOO^-$ was 24.0 nM according to the 3σ/slope. Clearly, the obtained results demonstrated that probe **NIR-HO** performed excellent sensitivity, effectiveness and potential applications for detection of Hg^{2+}-induced $ONOO^-$ generation. To examine the practical applicability **NIR-HO** in different pH PBS buffer, the fluorescence response of **NIR-HO** toward Hg^{2+} and $ONOO^-$ at different pH was explored (Figure S6). The probe **NIR-HO** showed faint and stabile fluorescence emission with different pH, even if mercury ions and $ONOO^-$ were added separately. While upon addition of both Hg^{2+} and $ONOO^-$, fluorescence emission

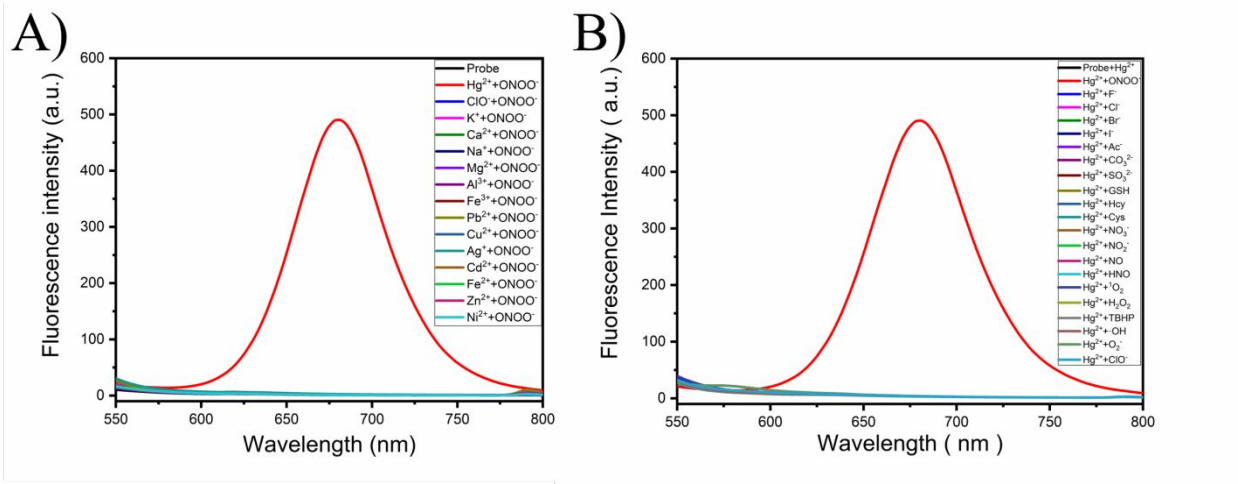

Figure 2. A) The fluorescence emission spectra of **NIR-HO** (10 μM) responded to other analytes (10 equiv.) in the presence of 10 equiv. Hg^{2+}. B) The fluorescence emission spectra of probe **NIR-HO** (10 μM) responded to 10 equiv. $ONOO^-$ in the presence of 10 equiv. other metal ions. (Ex = 550 nm)

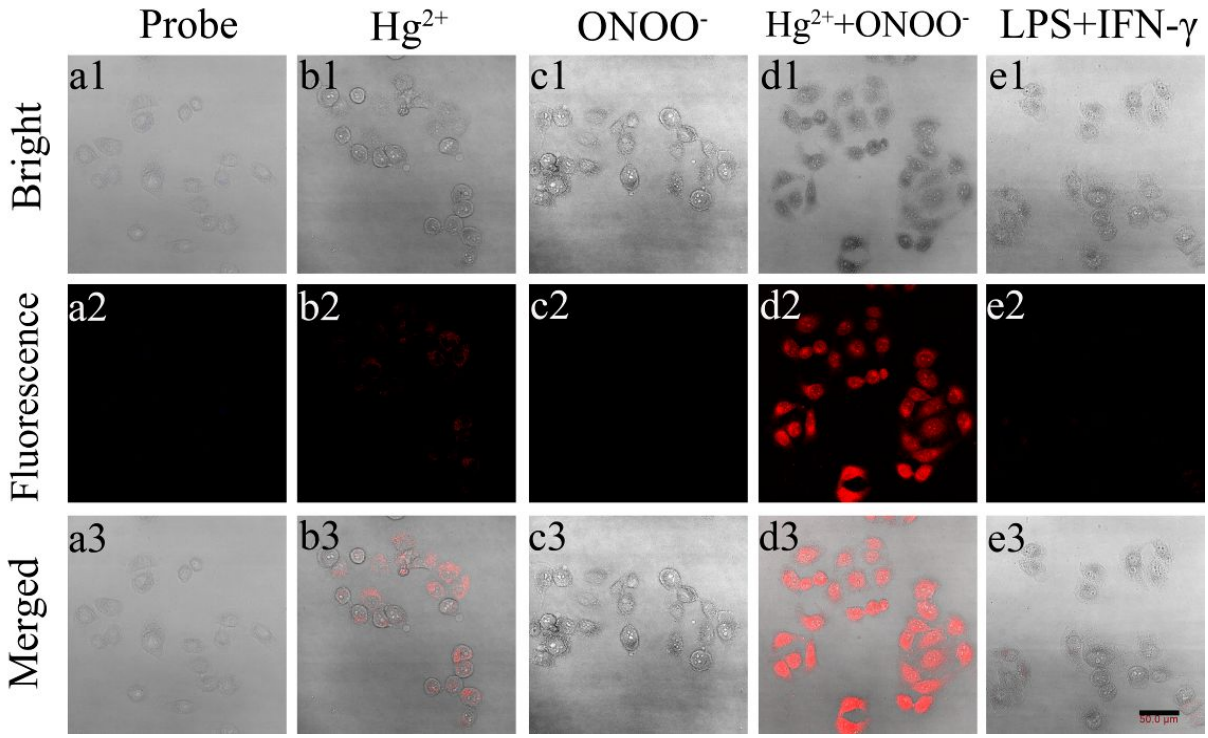

Figure 3. Fluorescence images of **NIR-HO** towards Hg^{2+} and $ONOO^-$ in MCF-7 cells. (a1-3) treated with NIR-HO (10 μM, 0.5 hour). (b1-3) pretreated with **NIR-HO** (10 μM, 0.5 hour) then incubated with Hg^{2+} (10 μM, 0.5 hour). (c1-3) treated with **NIR-HO** (10 μM, 0.5 hour) then incubated with $ONOO^-$ (100 μM, 0.5 hour). (d1-4) pretreated with **NIR-HO** (10 μM, 0.5 hour), then incubated with Hg^{2+} (100 μM) and $ONOO^-$ (100 μM) for 0.5 hour. (e1-3) pretreated with (LPS) and IFN-γ for 24 hour, then treated with **NIR-HO** (10 μM) for 0.5 hour. (a3-e3) Merged images of a1-e1 and a2-e2. (Excitation: 552 nm, emission: 640-720 nm, Scale bar: 50 μm).

intensity was significantly increased across a range of pH from 6.0 to 12.0, suggesting that the probe **NIR-HO** can be applied to physiological environment.

To test the selectivity and specificity of probe NIR-HO in complex biological system. The probe NIR-HO was firstly treated with various potentially activated species (ClO^-, K^+, Ca^{2+}, Na^+, Mg^{2+}, Al^{3+}, Fe^{3+}, Pb^{2+}, Cu^{2+}, Ag^+, Cd^{2+}, Fe^{2+}, Zn^{2+}, Ni^{2+}) and $ONOO^-$. As illustrated in Figure 2A, there was no significantly fluorescence emission changed at 680 nm. Similarly, upon treated with Hg^{2+} and other biologically relevant species (F^-, Cl^-, Br^-, I^-, AcO^-, CO_3^{2-}, SO_3^{2-}, GSH, Hcy, Cys, NO_3^-, NO_2^-, NO, HNO, $^1O_2$, H_2O_2, TBHP, ·OH, $O_2^{\cdot-}$, ClO^-), Figure 2B also presented no obvious change of fluorescence emission intensity. With this just the opposite is, probe **NIR-HO** only opened strong fluorescence emission after the addition of both Hg^{2+} and $ONOO^-$. The competitive binding assay revealed that the $ONOO^-$ induced fluorescence response was not affected by other interferences (Figure S7). Additionally, the influence of biologically relevant species on the UV performance of probe **NIR-HO** toward Hg^{2+} and $ONOO^-$ was also discussed (Figure S8). It can be found that biologically relevant species showed negligible interference for the detection of Hg^{2+} and $ONOO^-$. These preliminary results

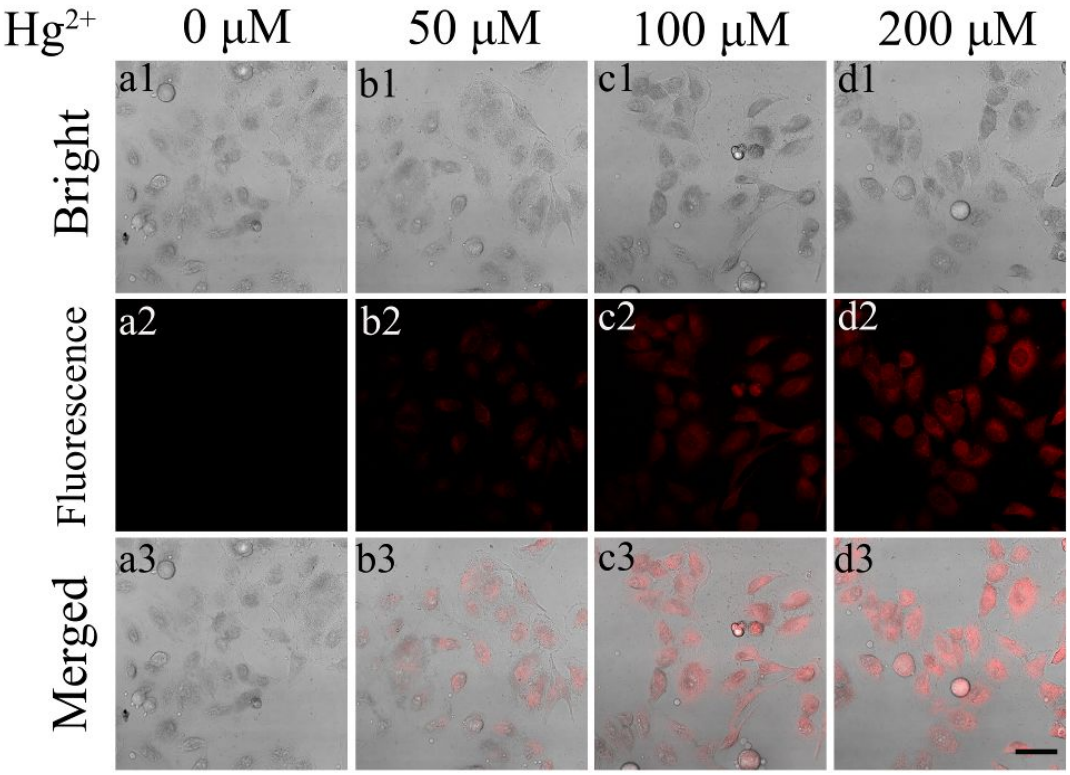

Figure 4. Fluorescence images of Hg^{2+}-induced oxidative stress with probe **NIR-HO** in MCF-7 cells. (a-d) Cells treated with different concentration of Hg^{2+} (0, 50, 100, 200 μM) for 1 hour, followed treatment with **NIR-HO** (10 μM) for 0.5 hour. (a3-d3) Merged images of a1-d1 and a2-d2. (Excitation: 552 nm, emission: 640-720 nm, Scale bar: 50 μm).

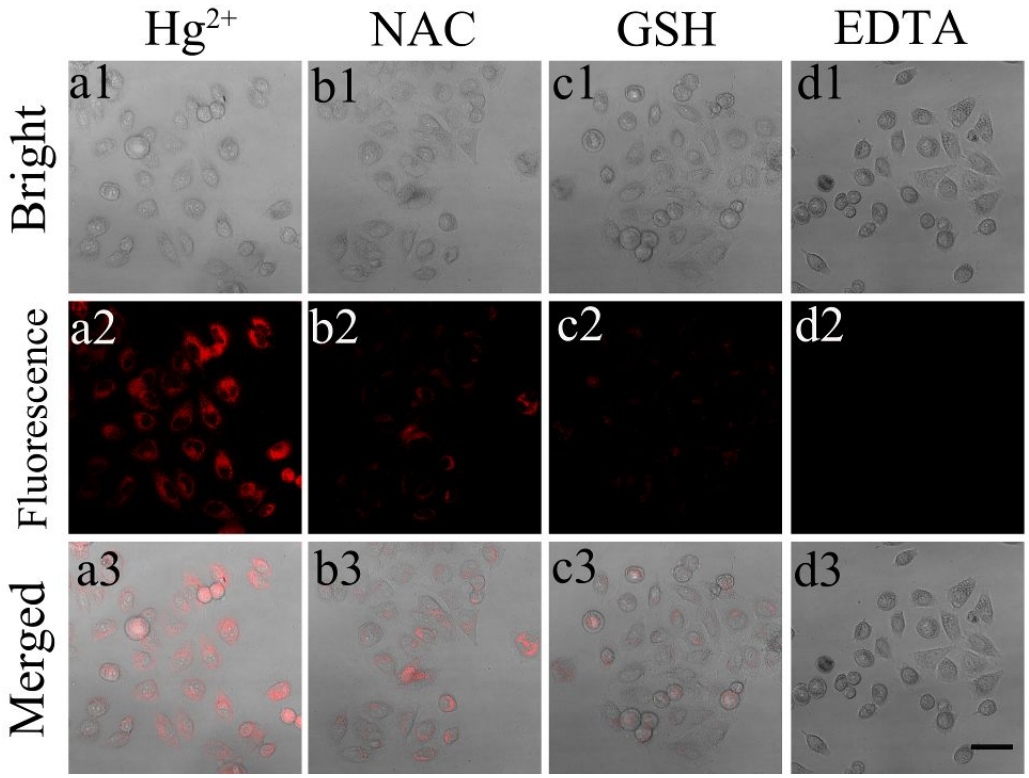

Figure 5. Fluorescence images of NIR-HO for Hg^{2+}-induced oxidative stress in MCF-7 cells. (a1-a3) cells with Hg^{2+} (200 μM) for 1 hour, subsequently treated with NIR-HO (10 μM, 0.5 hour). (b1-b3) cells were pretreated with NAC (1.0 mM, 1 h), then exposed to Hg^{2+} (200 μM), treatment with NIR-HO (10 μM, 0.5 hour); (c1-c3) pretreated with GSH (1.0 mM, 1 h), then exposed to Hg^{2+} (200 μM), treatment with NIR-HO (10 μM, 0.5 hour); (d1-d3) pretreated with EDTA (1.0 mM, 1 h), then exposed to Hg^{2+} (200 μM), treatment with NIR-HO (10 μM, 0.5 hour); (a3-d3) Merged images of a1-d1 and a2-d2. (Excitation: 552 nm, emission: 640-720 nm, Scale bar: 50 μm).

indicated high specificity and selectivity of **NIR-HO** to detect Hg^{2+} and $ONOO^-$ with "dual-key-and-lock" strategy.

Sensing mechanism. The possible recognition process was shown in Scheme 1, and the P=S of probe **NIR-HO** was firstly oxidized to P=O by Hg^{2+} because of its strong oxidation. The intermediate product **NIR-Hg** (calcd m/z 513.1702, $C_{31}H_{27}N_2NaO_2P^+$) was found in the HR-MS spectrum with a peak at m/z 513.1714 (Figure S9). Subsequently, the P-O of **NIR-Hg** was broken by $ONOO^-$, which generated the obvious fluorescence emission of **NIR-ONOO**. The founded peaks at m/z 289.1348 ($C_{19}H_{17}N_2O^-$) belonged to **NIR-ONOO** (calcd m/z 289.1346) (Figure S10). Generally, due to the series reaction of Hg^{2+} and $ONOO^-$ with the probe **NIR-HO**, the ICT system was then enhanced and released strong fluorescence signal, suggesting that probe **NIR-HO** was designed in line with "dual-key-and-lock" strategy.

Cell imaging. Inspired by the exceptional spectrum results of probe (Figure S11-12), we continued to investigate the application of **NIR-HO** toward Hg^{2+} and $ONOO^-$ in the biological environment. We first evaluated the cytotoxicity of **NIR-HO** using MCF-7 cells. The cell cytotoxicity was calculated by CCK-8 analysis through treating cells with **NIR-HO** (0-20 μM) for 24 hours. Those results indicated that cell viability had remained 90% after incubation of cells for 24 hours, as shown in Figure S13, demonstrating that **NIR-HO** has low cytotoxicity for cell imaging.

Subsequently, cells which were first incubated with **NIR-HO** showed a negligible fluorescence signal (Figure 3a). Upon treated with Hg^{2+}, cells revealed a little fluorescence enhancement due to Hg^{2+}-induced $ONOO^-$ generation (Figure 3b). When cells were treated with $ONOO^-$, negligible fluorescence signal was existed (Figure 3c). In sharp contrast, when cells were incubated with Hg^{2+} and $ONOO^-$, a significant fluorescence increase could be observed (Figure 3d), indicating that simultaneous stimulation of Hg^{2+} and $ONOO^-$ on the probe can contribute to fluorescence signal increase. After addition of LPS and IFN-γ for 24 hours, cells can endogenously generate $ONOO^-$. Then, cultured with **NIR-HO** for another 0.5 hour, cells showed a negligible change of fluorescence (Figure 3e). The results showed that **NIR-HO** can respond to Hg^{2+} and $ONOO^-$ with excellent selectivity and sensitivity in cells, and did not respond to other processes which induced oxidative stress in cells.

Normally, Hg belongs to one of the most toxic heavy metals, which can cause kidney, liver and nervous system poisoning. Although, lots of studies have been conducted on Hg-induced toxicity, its mechanism has not been fully elucidated. Oxidative stress may be closely related to Hg-induced toxicity. Therefore, Hg^{2+}-induced oxidative stress was real-time monitoring in cells by using the **NIR-HO** for Hg^{2+} and $ONOO^-$ detection. As presented in Figure 4a-d, cells incubated with **NIR-HO**, a weak fluorescence signal could be observed. As our expectation, when cells were exposed to increasing concentrations of Hg^{2+}, displayed significant fluorescent signal increasing. In order to study if **NIR-HO** dynamically monitoring the production of $ONOO^-$ by Hg^{2+}-induced oxidative stress, we recorded fluorescence signal changes at different time points. Cells were first cultured with the **NIR-HO**, then imaged. As the Figure S14 shows, fluorescence signal of cells did not change significantly which were incubated with PBS only. However, when Hg^{2+} was used to stimulate cells, a fluorescence intensity augmentation was observed in a short period of time, indicating that $ONOO^-$- related oxidative stress showed up after Hg^{2+} administration. Consequently, the results demonstrated that **NIR-HO** can be appropriate for monitoring Hg^{2+}-induced oxidative stress in living cells.

The toxicity of mercury ions shows a major threat to human health. Therefore, it is of great significance to find mercury detoxification drugs. Accordingly, GSH and NAC may effectively combined with Hg^{2+} to reduce its concentration, and deplete ROS and RNS levels in cells. EDTA is a good mercury ion chelator, which may efficiently induce decrease of Hg^{2+} level in cells. Therefore, in order to protect the cells from Hg^{2+} damage, we attempt to use NAC, GSH and EDTA as mercury detoxification drug based on the Hg^{2+}-induced toxicity mechanism. As shown in Figure 5a, **NIR-HO** loaded cells showed enhanced fluorescence signal after stimulated with Hg^{2+}. However, upon stimulation of these drugs NAC, GSH and EDTA, intracellular fluorescence signal in cells gradually decreased (Figure 5b-d). As a result, the results confirmed that NAC, GSH and EDTA can be potentially employed as a detoxifying drugs for remedy Hg^{2+}-induced toxicity.

In vivo imaging. Finally, we further investigated the feasibility of **NIR-HO** for visualizing Hg^{2+} and $ONOO^-$ in Kunming mice motivated by its NIR fluorescence emission. Based on Figure 6, the mice displayed faint fluorescence emission in NIR emission channel which was subcutaneously injected with only **NIR-HO**. In another group, obvious fluorescence emission enhancement was observed after given a subcutaneous injection of **NIR-HO**, then an injection of Hg^{2+} and $ONOO^-$ stock solution 0.5 hour later. Therefore, this suggested that **NIR-HO** can be applied to image Hg^{2+} and $ONOO^-$ in vivo.

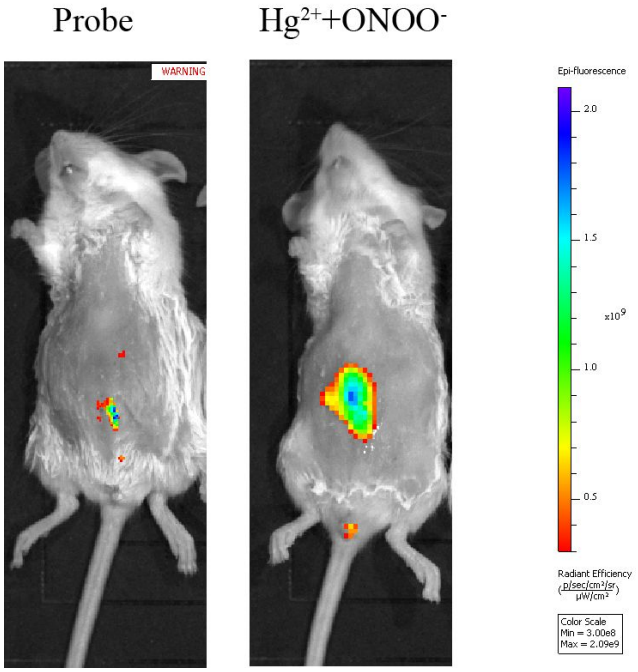

Figure 6. Fluorescent images of **NIR-HO** in vivo. Left: Mice were injected with **NIR-HO** (100 μL, 10 μM) for 0.5 hour, subcutaneously injected PBS buffer (100 μL left), then imaged. Right: mice were injected Hg^{2+} and $ONOO^-$ (100 μL, 10 μM) for 0.5 hour, then imaged. (550-nm excitation and 680-nm emission).

CONCLUSIONS

To conclude, we have reported a new type of Hg^{2+}-activated and NIR emission fluorescent probe **NIR-HO** for detecting $ONOO^-$ with "dual-key-and-lock" strategy. The probe **NIR-HO** showed excellent specificity and sensitivity for detecting Hg^{2+} and $ONOO^-$ in vitro and cells. In addition, it was proved that Hg^{2+} could damage the body's antioxidant defense system function, causing the occurrence of $ONOO^-$ level upregulation. Therefore,

oxidative stress may be the main pathogenic mechanism in mercury-induced toxicity. More importantly, it was found that NAC, GSH, and EDTA were employed as an excellent detoxifying drug against Hg^{2+}-induced toxicity. The new probe may provide an effective method for detecting Hg^{2+}- oxidative stress detection and studying the development of detoxifying drugs.

ASSOCIATED CONTENT

Supporting Information

The details of apparatus, materials, ^{1}H NMR, ^{13}C NMR, and HR-MS spectra; fluorescent and UV spectroscopic data, cytotoxicity assay, bioimaging could be found in supporting information, which is available free of charge on the ACS Publications website.

AUTHOR INFORMATION

Corresponding Author

*E-mail: yeyong03@tsinghua.org.cn. Tel: +86-371-67767050. Fax: +86-371-67767051. pandy811@163.com

ORCID

Yong Ye: 0000-0001-6234-3971

Notes

The authors declare no competing financial interests.

ACKNOWLEDGMENT

This work was financially supported by the National Science Foundation of China (No. 21572209 and 21907025), Scientific and Technological Project of Henan Province of China (192102310140), Scientific and Technological Innovation Project of Henan Academy of Agricultural Sciences(2020CX05)

REFERENCES

(1). Zhang, X. L.; Xiao, Y.; Qian, X. H., A Ratiometric Fluorescent Probe Based on FRET for Imaging Hg^{2+} Ions in Living Cells. *Angew. Chem. Int. Ed.* **2008,** *47*, 8025-8029.

(2). Yan, F.; Cao, D.; Yang, N.; Yu, Q.; Wang, M.; Chen, L., A selective turn-on fluorescent chemosensor based on rhodamine for Hg^{2+} and its application in live cell imaging. *Sensors Actuators B: Chem.* **2012,** *162*, 313-320.

(3). Wang, F.; Nam, S.-W.; Guo, Z.; Park, S.; Yoon, J., A new rhodamine derivative bearing benzothiazole and thiocarbonyl moieties as a highly selective fluorescent and colorimetric chemodosimeter for Hg^{2+}. *Sensors Actuators B: Chem.* **2012,** *161*, 948-953.

(4). Santra, M.; Roy, B.; Ahn, K. H., A "Reactive" Ratiometric Fluorescent Probe for Mercury Species. *Org. Lett.* **2011,** *13*, 3422-3425.

(5). Hayes, J. D.; Flanagan, J. U.; Jowsey, I. R., Glutathlone Transferases. **2005,** *45*, 51-88.

(6). Wang, Y.; Zhang, L.; Chen, L., Glutathione Peroxidase-Activatable Two-Photon Ratiometric Fluorescent Probe for Redox Mechanism Research in Aging and Mercury Exposure Mice Models. *Anal. Chem.* **2020**, 92, 1997-2004.

(7). Wang, Y.; Gao, M.; Chen, Q.; Yu, F.; Jiang, G.; Chen, L., Associated Detection of Superoxide Anion and Mercury(II) under Chronic Mercury Exposure in Cells and Mice Models via a Three-Channel Fluorescent Probe. *Anal. Chem.* **2018,** *90*, 9769-9778.

(8). Wang, Y.; Gao, M.; Liao, C.; Yu, F.; Chen, L., A sulfydryl-based near-infrared ratiometic fluorescent probe for assessment of acute/chronic mercury exposure via associated determination of superoxide anion and mercury ion in cells and in vivo. *Sensors Actuators B: Chem.* **2019,** *301*, 127038.

(9). Farina, M.; Avila, D. S.; da Rocha, J. B. T.; Aschner, M., Metals, oxidative stress and neurodegeneration: A focus on iron, manganese and mercury. *Neurochem. Int.* **2013,** *62*, 575-594.

(10). Szabó, C., The pathophysiological role of peroxynitrite in shock, inflammation, and ischemia-reperfusion injury. *Shock* **1996,** *6*, 79-88.

(11). Zhang, W.; Liu, J.; Li, P.; Wang, X.; Bi, S.; Zhang, J.; Zhang, W.; Wang, H.; Tang, B., In situ and real-time imaging of superoxide anion and peroxynitrite elucidating arginase 1 nitration aggravating hepatic ischemia-reperfusion injury. *Biomaterials* **2019,** *225*, 119499.

(12). Chen, X.; Wang, F.; Hyun, J. Y.; Wei, T.; Qiang, J.; Ren, X.; Shin, I.; Yoon, J., Recent progress in the development of fluorescent, luminescent and colorimetric probes for detection of reactive oxygen and nitrogen species. *Chem.Soc. Rev.* **2016,** *45*, 2976-3016.

(13). Tsai, J.-H. M.; Harrison, J. G.; Martin, J. C.; Hamilton, T. P.; van der Woerd, M.; Jablonsky, M. J.; Beckman, J. S., Role of Conformation of Peroxynitrite Anion ($ONOO^-$) with Its Stability and Toxicity. *J. Am. Chem. Soc.* **1994,** *116*, 4115-4116.

(14). Li, X.; Zhu, F.; He, Y.; Luo, F., Arginase inhibitor nor-NOHA induces apoptosis and inhibits invasion and migration of HepG2 cells. *Chin. J. Cell. Mol. Immunol.* **2017,** *33*, 477-482.

(15). Hecker, M.; Nematollahi, H.; Hey, C.; Busse, R.; Racké, K., Inhibition of arginase by in alveolar macrophages: implications for the utilization of l-arginine for nitric oxide synthesis. *FEBS Lett.* **1995,** *359* (2-3), 251-254.

(16). Hey, C.; Boucher, J. L.; Goff, F. V. L.; Ketterer, G.; Wessler, I.; Racke, K., Inhibition of arginase in rat and rabbit alveolar macrophages by N-omega-hydroxy-D,L-indospicine, effects on L-arginine utilization by nitric oxide synthase. *Br. J. Pharmacol.* **1997,** *121*, 395-400.

(17). Ferrer-Sueta, G.; Campolo, N.; Trujillo, M.; Bartesaghi, S.; Carballal, S.; Romero, N.; Alvarez, B.; Radi, R., Biochemistry of Peroxynitrite and Protein Tyrosine Nitration. *Chem. Rev.* **2018,** *118*, 1338-1408.

(18). Cheng, J.; Li, D.; Sun, M.; Wang, Y.; Xu, Q.-Q.; Liang, X.-G.; Lu, Y.-B.; Hu, Y.; Han, F.; Li, X., Physicochemical-property guided design of a highly sensitive probe to image nitrosative stress in the pathology of stroke. *Chem.l Sci.* **2020,** *11*, 281-289.

(19). Radi, R., Oxygen radicals, nitric oxide, and peroxynitrite: Redox pathways in molecular medicine. *Proc. Natl. Acad. Sci. U. S. A.* **2018,** *115*, 5839-5848.

(20). Cheng, D.; Pan, Y.; Wang, L.; Zeng, Z.; Yuan, L.; Zhang, X.; Chang, Y.-T., Selective Visualization of the Endogenous Peroxynitrite in an Inflamed Mouse Model by a Mitochondria-Targetable Two-Photon Ratiometric Fluorescent Probe. *J. Am. Chem. Soc.***2017,** *139*, 285-292.

(21). Huang, J.; Li, J.; Lyu, Y.; Miao, Q.; Pu, K., Molecular optical imaging probes for early diagnosis of drug-induced acute kidney injury. *Nat. Mater.* **2019,** *18*, 1133-1143.

(22). Xie, X.; Tang, F.; Liu, G.; Li, Y.; Su, X.; Jiao, X.; Wang, X.; Tang, B., Mitochondrial Peroxynitrite Mediation of Anthracycline-Induced Cardiotoxicity as Visualized by a Two-Photon Near-Infrared Fluorescent Probe. *Anal. Chem.***2018,** *90*, 11629-11635.

(23). Zhang, J. J.; Zhen, X.; Upputuri, P. K.; Pramanik, M.; Chen, P.; Pu, K. Y., Activatable Photoacoustic Nanoprobes for In Vivo Ratiometric Imaging of Peroxynitrite. *Adv. Mater.* **2017,** *29*, 1604764.

(24). Ren, M.; Wang, L.; Lv, X.; Liu, J.; Chen, H.; Wang, J.; Guo, W., Development of a benzothiazole-functionalized red-emission pyronin dye and its dihydro derivative for imaging lysosomal viscosity and tracking endogenous peroxynitrite. *J. Mater.Chem.B* **2019,** *7*, 6181-6186.

(25). Chen, Y.; Bi, K. Y.; Hao, R. T.; Xie, P.; Huang, L. N.; Wang, Y. M.; Zhang, J. F.; Xu, R.; Wu, X. H., Near-Infrared Ratiometric Fluorescent Probe for Detection of Peroxynitrite in HeLa Cells Based on Dicyanomethylene-4H-pyran Coumarin System. *Chin. J. Org. Chem.* **2020,** *40*, 511-515.

(26). Chen, X.; Tian, X.; Shin, I.; Yoon, J., Fluorescent and luminescent probes for detection of reactive oxygen and nitrogen species. *Chem. Soc. Rev.* **2011,** *40*, 4783-4804.

(27). Emanuele, S.; D'Anneo, A.; Calvaruso, G.; Cernigliaro, C.; Giuliano, M.; Lauricella, M., The Double-Edged Sword Profile of Redox Signaling: Oxidative Events As Molecular Switches in the Balance between Cell Physiology and Cancer. *Chem.Res. Tox.* **2018,** *31*, 201-210.

(28). Hu, J. S.; Shao, C. W.; Wang, X. A.; Di, X. J.; Xue, X. L.; Su, Z.; Zhao, J.; Zhu, H. L.; Liu, H. K.; Qian, Y., Imaging Dynamic Peroxynitrite Fluxes in Epileptic Brains with a Near-Infrared Fluorescent Probe. *Adv. Sci.* **2019,** *6*, 1900341.

(29). Wu, L.; Sedgwick, A. C.; Sun, X.; Bull, S. D.; He, X.-P.; James, T. D., Reaction-Based Fluorescent Probes for the Detection and Imaging of

Reactive Oxygen, Nitrogen, and Sulfur Species. *Acc. Chem. Res.* **2019,** *52* , 2582-2597.
(30). Yue, Y.; Huo, F.; Cheng, F.; Zhu, X.; Mafireyi, T.; Strongin, R. M.; Yin, C., Functional synthetic probes for selective targeting and multi-analyte detection and imaging. *Chem. Soc. Rev.* **2019,** *48*, 4155-4177.
(31). Yang, X.; Liu, W.; Tang, J.; Li, P.; Weng, H.; Ye, Y.; Xian, M.; Tang, B.; Zhao, Y., A multi-signal mitochondria-targeted fluorescent probe for real-time visualization of cysteine metabolism in living cells and animals. *Chem. Commun.* **2018,** *54*, 11387-11390.
(32). Zhang, D.; Chen, W.; Miao, Z.; Ye, Y.; Zhao, Y.; King, S. B.; Xian, M., A reductive ligation based fluorescent probe for S-nitrosothiols. *Chem. Commun.* **2014,** *50*, 4806-4809.
(33). Zhang, B.; Yang, X.; Zhang, R.; Liu, Y.; Ren, X.; Xian, M.; Ye, Y.; Zhao, Y., Lysosomal-Targeted Two-Photon Fluorescent Probe to Sense Hypochlorous Acid in Live Cells. *Anal. Chem.* **2017,** *89*, 10384-10390.
(34). Wang, L.; Liu, J.; Zhao, S.; Zhang, H.; Sun, Y.; Wei, A.; Guo, W., Fluorescence imaging of hypochlorous acid and peroxynitrite in vitro and in vivo with emission wavelength beyond 750 nm. *Chem. Commun.* **2020**, *56*, 7718-7721.
(35). Wen, Y.; Huo, F. J.; Yin, C. X., Organelle targetable fluorescent probes for hydrogen peroxide. *Chin. Chem. Lett.* **2019,** *30*, 1834-1842.
(36). Zhang, B.; Zhang, H.; Zhong, M.; Wang, S.; Xu, Q.; Cho, D.-H.; Qiu, H., A novel off-on fluorescent probe for specific detection and imaging of cysteine in live cells and in vivo. *Chin. Chem. Lett.* **2020,** *31*, 133-135.
(37). Zhu, J.; Qin, F.; Zhang, D.; Tang, J.; Liu, W.; Cao, W.; Ye, Y., A novel NIR fluorescent probe for the double-site and ratiometric detection of SO_2 derivatives and its applications. *New J. Chem.* **2019,** *43*, 16806-16811.
(38). Yang, X.; Wang, Y.; Liu, R.; Zhang, Y.; Tang, J.; Yang, E.; Zhang, D.; Zhao, Y.; Ye, Y., A novel ICT-based two photon and NIR fluorescent probe for labile Fe^{2+} detection and cell imaging in living cells. *Sensors Actuators B: Chem.***2019,** *288*, 217-224.
(39). Guo, Z.; Park, S.; Yoon, J.; Shin, I., Recent progress in the development of near-infrared fluorescent probes for bioimaging applications. *Chem. Soc. Rev.* **2014,** *43*, 16-29.
(40). Yuan, L.; Lin, W.; Zheng, K.; He, L.; Huang, W., Far-red to near infrared analyte-responsive fluorescent probes based on organic fluorophore platforms for fluorescence imaging. *Chem.Soc. Rev.* **2013,** *42* , 622-661.
(41). Huang, Y.; Qi, Y.; Zhan, C.; Zeng, F.; Wu, S., Diagnosing Drug-Induced Liver Injury by Multispectral Optoacoustic Tomography and Fluorescence Imaging Using a Leucine-Aminopeptidase-Activated Probe. *Anal. Chem.* **2019,** *91*, 8085-8092.
(42). Chen, S. H.; Pang, C. M.; Chen, X. Y.; Yan, Z. H.; Huang, S. M.; Li, X. D.; Zhong, Y. T.; Wang, Z. Y., Research Progress in Design, Synthesis and Application of Multifunctional Fluorescent Probes. *Chin. J. Org. Chem.* **2019,** *39*, 1846-1857.
(43). Wu, L. Y.; Zeng, W. H.; Feng, L. D.; Hu, Y. X.; Sun, Y. D.; Yan, Y. X.; Chen, H. Y.; Ye, D. J., An activatable ratiometric near-infrared fluorescent probe for hydrogen sulfide imaging in vivo. *Sci. China-Chem.* **2020,** *63*, 741-750.
(44). Murfin, L. C.; Weber, M.; Park, S. J.; Kim, W. T.; Lopez-Alled, C. M.; McMullin, C. L.; Pradaux-Caggiano, F.; Lyall, C. L.; Kociok-Köhn, G.; Wenk, J.; Bull, S. D.; Yoon, J.; Kim, H. M.; James, T. D.; Lewis, S. E., Azulene-Derived Fluorescent Probe for Bioimaging: Detection of Reactive Oxygen and Nitrogen Species by Two-Photon Microscopy. *J. Am. Chem. Soc.* **2019,** *141*, 19389-19396.
(45). Zhou, D.-Y.; Li, Y.; Jiang, W.-L.; Tian, Y.; Fei, J.; Li, C.-Y., A ratiometric fluorescent probe for peroxynitrite prepared by de novo synthesis and its application in assessing the mitochondrial oxidative stress status in cells and in vivo. *Chem. Commun.* **2018,** *54*, 11590-11593.
(46). Yu, F.; Li, P.; Li, G.; Zhao, G.; Chu, T.; Han, K., A Near-IR Reversible Fluorescent Probe Modulated by Selenium for Monitoring Peroxynitrite and Imaging in Living Cells. *J. Am. Chem. Soc.* **2011,** *133*, 11030-11033.
(47). Han, R.; Yang, X.; Zhang, D.; Fan, M.; Ye, Y.; Zhao, Y., A bis(rhodamine)-based highly sensitive and selective fluorescent chemosensor for Hg(ii) in aqueous media. *New J. Chem.* **2012,** *36*, 1961-1965.
(48). Zhang, D.; Li, M.; Jiang, Y.; Wang, C.; Wang, Z.; Ye, Y.; Zhao, Y., A new sensitive and selective chromogenic and fluorescent chemodosimeter for Hg(Ⅱ) in aqueous media and its application in live cell imaging. *Dyes Pigm.* **2013,** *99*, 607-612.
(49). Cheng, D.; Peng, J.; Lv, Y.; Su, D.; Liu, D.; Chen, M.; Yuan, L.; Zhang, X., De Novo Design of Chemical Stability Near-Infrared Molecular Probes for High-Fidelity Hepatotoxicity Evaluation In Vivo. *J. Am. Chem. Soc.* **2019,** *141*, 6352-6361.
(50). Wu, W.; Zhang, C.; Rees, T. W.; Liao, X.; Yan, X.; Chen, Y.; Ji, L.; Chao, H., Lysosome-Targeting Iridium(III) Probe with Near-Infrared Emission for the Visualization of $NO/O_2^{\bullet-}$ Crosstalk via In Vivo Peroxynitrite Imaging. *Anal. Chem.* **2020,** *92*, 6003-6009.
(51). Neupane, L. N.; Park, J.; Mehta, P. K.; Oh, E.-T.; Park, H. J.; Lee, K.-H., Fast and sensitive fluorescent detection of inorganic mercury species and methylmercury using a fluorescent probe based on the displacement reaction of arylboronic acid with the mercury species. *Chem. Commun.* **2020,** *56*, 2941-2944.
(52). Li, Y.; Xie, X.; Yang, X.; Li, M.; Jiao, X.; Sun, Y.; Wang, X.; Tang, B., Two-photon fluorescent probe for revealing drug-induced hepatotoxicity via mapping fluctuation of peroxynitrite. *Chemi. Sci.* **2017,** *8*, 4006-4011.
(53). Zhang, H.; Liu, J.; Sun, Y.-Q.; Huo, Y.; Li, Y.; Liu, W.; Wu, X.; Zhu, N.; Shi, Y.; Guo, W., A mitochondria-targetable fluorescent probe for peroxynitrite: fast response and high selectivity. *Chem. Commun.* **2015,** *51*, 2721-2724.
(54). Miao, J.; Huo, Y.; Shi, H.; Fang, J.; Wang, J.; Guo, W., A Si-rhodamine-based near-infrared fluorescent probe for visualizing endogenous peroxynitrite in living cells, tissues, and animals. *J. Mater. Chem. B* **2018,** 6 , 4466-4473.
(55). Li, X.; Tao, R.-R.; Hong, L.-J.; Cheng, J.; Jiang, Q.; Lu, Y.-M.; Liao, M.-H.; Ye, W.-F.; Lu, N.-N.; Han, F.; Hu, Y.-Z.; Hu, Y.-H., Visualizing Peroxynitrite Fluxes in Endothelial Cells Reveals the Dynamic Progression of Brain Vascular Injury. *Journal of the American Chem. Soc.***2015,** *137*, 12296-12303.
(56). Yoon, S.; Miller, E. W.; He, Q.; Do, P. H.; Chang, C. J., A bright and specific fluorescent sensor for mercury in water, cells, and tissue. *Angew. Chem. Int. Ed.* **2007,** *46*, 6658-6661.
(57). Tian, J. W.; Chen, H. C.; Zhuo, L. H.; Xie, Y. X.; Li, N.; Tang, B., A Highly Selective, Cell-Permeable Fluorescent Nanoprobe for Ratiometric Detection and Imaging of Peroxynitrite in Living Cells. *Chem. Eur. J.* **2011,** *17*, 6626-6634.
(58). Sun, Q.; Xu, J.; Ji, C.; Shaibani, M. S. S.; Li, Z.; Lim, K.; Zhang, C.; Li, L.; Liu, Z., Ultrafast Detection of Peroxynitrite in Parkinson's Disease Models Using a Near-Infrared Fluorescent Probe. *Anal. Chem.* **2020,** *92* (5), 4038-4045.
(59). Oh, S.; Jeon, J.; Jeong, J.; Park, J.; Oh, E.-T.; Park, H. J.; Lee, K.-H., Fluorescent Detection of Methyl Mercury in Aqueous Solution and Live Cells Using Fluorescent Probe and Micelle Systems. *Anal. Chem.* **2020,** *92*, 4917-4925.
(60). Liu, C.; Zhang, R.; Zhang, W.; Liu, J.; Wang, Y.-L.; Du, Z.; Song, B.; Xu, Z. P.; Yuan, J., "Dual-Key-and-Lock" Ruthenium Complex Probe for Lysosomal Formaldehyde in Cancer Cells and Tumors. *J. Am. Chem. Soc.* **2019,** *141*, 8462-8472.
(61). Liu, Y.; Teng, L.; Xu, C.; Liu, H.-W.; Xu, S.; Guo, H.; Yuan, L.; Zhang, X.-B., A "Double-Locked" and enzyme-activated molecular probe for accurate bioimaging and hepatopathy differentiation. *Chem. Sci.* **2019,** *10*, 10931-10936.
(62). Teng, L.; Song, G.; Liu, Y.; Han, X.; Li, Z.; Wang, Y.; Huan, S.; Zhang, X.-B.; Tan, W., Nitric Oxide-Activated "Dual-Key–One-Lock" Nanoprobe for in Vivo Molecular Imaging and High-Specificity Cancer Therapy. *J. Am. Chem. Soc.* **2019,** *141*, 13572-13581.
(63). Zhang, Y. T.; Yan, C. X.; Wang, C.; Guo, Z. Q.; Liu, X. G.; Zhu, W. H., A Sequential Dual-Lock Strategy for Photoactivatable Chemiluminescent Probes Enabling Bright Duplex Optical Imaging. *Angew. Chem. Int. Ed.* **2020,** *59*, 9059-9066.
(64). Im, H. G.; Kim, H. Y.; Chang, S.-K., Dual signaling of Hg^{2+} ions by selective cleavage of thiophosphinated rhodol. *Sensors and Actuators B: Chemical* **2014,** *191*, 854-859.
(65). Yuan, R.; Ma, Y.; Du, J.; Meng, F.; Guo, J.; Hong, M.; Yue, Q.; Li, X.; Li, C., A novel highly selective near-infrared and naked-eye fluorescence probe for imaging peroxynitrite. *Anal. Methods* **2019,** *11*, 1522-1529.
(66). Wu, Y.; Shi, A.; Li, Y.; Zeng, H.; Chen, X.; Wu, J.; Fan, X., A near-infrared xanthene fluorescence probe for monitoring peroxynitrite in living cells and mouse inflammation model. *Analyst* **2018,** *143*, 5512-5519.
(67). Wagner, J.; Ciesielski, M.; Fleckenstein, C. A.; Denecke, H.; Garlichs, F.; Ball, A.; Doering, M., Benign and High-Yielding, Large-

Scale Synthesis of Diphenylphosphinodithioic Acid and Related Compounds. *Org. Process Res. Dev.* **2013,** *17*, 47-52.
(68). Wang, C.; Wang, Y.; Wang, G.; Chen, S.; Huang, C., Two-isophorone fluorophore-based design of a ratiometric fluorescent probe and its application in the sensing of biothiols. *J. Mater. Chem. B* **2019,** *7*, 5633-5639.

For TOC only